ARTICLES

Sensing Behaviors of Polypyrrole Nanotubes Prepared in Reverse Microemulsions: Effects of Transducer Size and Transduction Mechanism

Hyeonseok Yoon, Mincheol Chang, and Jyongsik Jang*

Hyperstructured Organic Materials Research Center, School of Chemical Engineering, College of Engineering, Seoul National University, Shinlimdong 56-1, Seoul 151-742, Korea

Received: March 8, 2006; In Final Form: May 16, 2006

Polypyrrole (PPy) nanotubes with different diameters were readily fabricated using cylindrical micelle templates in sodium bis(2-ethylhexyl) sulfosuccinate (AOT) reverse microemulsions. Interestingly, Raman spectroscopy and ultraviolet (UV)−visible spectroscopy revealed that the PPy nanotubes with smaller diameters had a more extended conjugation length as well as a higher oxidation level. The PPy nanotubes were deposited onto a microelectrode array and were exposed to chemical vapor and electromagnetic radiation: typically, NH_3 vapor and UV light were chosen. The electrical response of PPy nanotubes to two different kinds of analytes was strongly dependent on their diameters. Moreover, since the small dimensions of PPy nanotubes facilitated the interaction between nanotubes and analytes, the PPy nanotube sensors showed conspicuously enhanced responses compared with conventional PPy.

Introduction

One of the most noteworthy abilities of conducting polymers is to recognize certain analytes through their inherent signal transduction mechanisms.[1−3] Various kinds of conducting polymers including polypyrrole (PPy), polyaniline, and polythiophene have been applied to sensor devices in order to detect diverse analytes such as toxic gases, volatile organic compounds, and biological species.[4] Wang et al. demonstrated the feasibility of PPy/polyetherurethane composite foams as the chemical sensor for volatile amines.[5] In addition, Li et al. electrophoretically deposited polyaniline colloids onto the sensing elements within a sensor array and investigated their sensitivity to gaseous analytes including water and methanol.[6] In recent years, conducting polymer materials of nanometer sizes have received considerable attention as promising candidates for fabricating state-of-the-art sensor devices.[7−9] For example, several different kinds of polyaniline nanofibers have been employed as sensing materials for the recognition of acids, bases, and organic vapors.[10−13] In addition, polypyrrole nanowires were patterned between gold microelectrodes on a silicon substrate through a lift-off process and used to detect ammonia gas.[14] Nevertheless, it is still challenging to realize nanomaterial-based sensors for practical applications because of the difficulty in synthesizing and manipulating the nanomaterials.

Until now, a hard template approach using porous templates (e.g., anodic aluminum oxide and track-etched polycarbonate membranes) has been the most frequent synthetic method for fabricating one-dimensional (1D) nanostructures.[15] This approach has the advantage of producing nanotubes and nanofibers with uniform diameters and lengths. Thus, various 1D conducting polymer nanomaterials consisting of PPy, polyaniline, poly(3,4-ethylenedioxythiophene), and so forth have been synthesized by chemical or electrochemical polymerization inside the cylindrical pores of hard templates.[16−19] However, the hard template approach involves a serious drawback that products can be obtained only in small quantities despite its complicated synthetic process. To this end, a soft template approach has appeared as an alternative tool to effectively fabricate 1D nanostructures.[20−22] This approach is relatively adaptable to large-scale synthesis and it is possible to control the morphology of 1D nanostructures by varying synthetic variables.[23−26] Recently, we have developed a facile and effective methodology to fabricate PPy nanotubes in sodium bis(2-ethylhexyl) sulfosuccinate (AOT) micelle systems.[27] Herein, we explored the electrical response of PPy nanotubes to ammonia (NH_3) vapor and ultraviolet (UV) light via distinct transduction mechanisms. In addition, we investigated the effect of the nanotube size on their sensitivity to the analytes.

Experimental Methods

PPy nanotubes could be prepared by the AOT cylindrical micelle templating with 7 M aqueous $FeCl_3$ solution in hexane at 15 °C.[27] A microarray consisting of a pair of gold interdigitated electrodes with 40 fingers (50 nm thickness on a 50 nm Cr adhesion layer) was patterned on a glass substrate through a photolithographic process (Figure 1). A 0.1 mL volume of ethanol solution containing 1 wt % PPy nanotubes was deposited onto the microelectrode, and then the sensor substrate was dried in a vacuum oven at room temperature to remove residual solvents. The normalized electrical resistance change (defined as $\Delta R/R_0 = (R - R_0)/R_0$, where R and R_0 denote the real-time resistance and initial resistance) of the sensor substrate was examined to measure the sensitivity of PPy nanotubes upon exposure to NH_3 vapor and UV light. The resistance change

* Corresponding author. Telephone: 82-2-880-7069. Fax: 82-2-888-7295. E-mail: jsjang@plaza.snu.ac.kr.

10.1021/jp061423b CCC: $33.50
Published on Web 07/04/2006

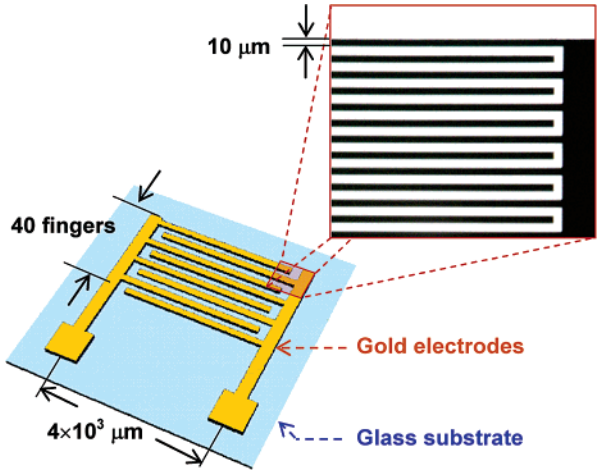

Figure 1. Schematic illustration and optical micrograph of a gold microelectrode array on glass substrate (finger dimensions: 10 μm width, 50 nm thickness, 4 × 10^3 μm length, 10 μm interelectrode spacing).

was monitored at room temperature in real time with a Keithley 2400 source meter. The PPy nanotubes were periodically exposed to NH_3/air stream in order to evaluate the reversibility and reproducibility of the sensors. The sensor substrate was put in a testing chamber (350 mL) with a gas inlet/outlet. After NH_3 vapor (20, 50, and 100 ppm) was injected into the chamber, it was replaced by compressed air (20% relative humidity). This process was repeated several times. The NH_3/air stream was supplied at a flow rate of 3 L min^{-1}. To investigate the sensitivity of PPy nanotubes upon exposure to NH_3 vapor, the sensor substrate was placed in a vacuum chamber maintained at 1 Torr, and 0.01 mL of NH_3 vapor (10−100 ppm) was injected into the chamber. The sensitivity of PPy nanotubes was determined as the normalized resistance change measured after the 200-s exposure to NH_3 vapor. To examine the effect of UV light irradiation on the nanotube conductivity, the sensor substrate was illuminated with high-intensity (8900 μW cm^{-2} at 10 in.) long-wave UV light from a UVP BLAK-RAY B-100AP lamp held at a fixed distance of 10 cm. The photosensitivity of the nanotubes was defined as the normalized resistance change recorded after the UV light irradiation.

Results and Discussion

The average diameters of PPy nanotubes prepared with AOT concentrations of 39.1 × 10^{-2} and 27.5 × 10^{-2} M were 96 ± 12 nm (PNT-1) and 194 ± 46 nm (PNT-2), respectively. Figure 2 exhibits the Raman spectra of PPy nanotubes in the range of 600−1800 cm^{-1}. The 1590 and 1487 cm^{-1} bands are attributed to the C=C backbone stretching in the oxidized (doped) and reduced (dedoped) PPy, respectively. As the conjugation length extends, the intensity of the band at 1590 cm^{-1} increases relative to the intensity of the band at 1487 cm^{-1}.[28] In Figure 2, the intensity ratio of the band at 1590 cm^{-1} to the one at 1487 cm^{-1} (I_{1590}/I_{1487}) was 4.7 in PNT-1, whereas the value of I_{1590}/I_{1487} was 4.2 in PNT-2. This fact indicates that PNT-1 has a relatively longer conjugation length than PNT-2. The conjugation length means the length of the polyene segment along which the delocalization of π-electrons takes place, and thus the conjugation length in conducting polymers is directly related to their conductivity. The conductivities of PNT-1 and PNT-2 were, respectively, 35 and 12 S cm^{-1}; the conductivity of PPy bulk was around 1 S cm^{-1}. Therefore, such a result was in good agreement with the higher conductivity of PNT-1 in comparison with that of PNT-2.

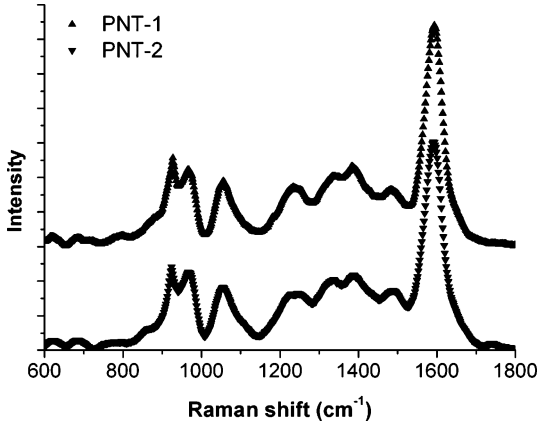

Figure 2. Raman spectra of PPy nanotubes with different diameters (PNT-1 and PNT-2).

The conductivity of PPy is susceptible to a chemical or electrochemical redox process, which involves the transfer of electrons and the exchange of counterions for the charge compensation on the polymer chain. In the electrically conductive state, PPy is a p-type semiconductor. As PPy is exposed to electron-donating molecules such as NH_3, a redox reaction can occur reversibly as shown by

$$PPy^+/Cl^- + NH_3(\delta^-) \underset{\text{oxidn}}{\overset{\text{redn}}{\rightleftharpoons}} PPy^0/NH_3(\delta^-)^+/Cl^- \quad (1)$$

The introduction of NH_3 into PPy nanotubes led to the formation of neutral polymer backbone from a positive-charged one and thus the decrease of charge-carrier concentration. These phenomena are necessarily accompanied by the decrease in conductivity of PPy nanotubes.

Figure 3a represents the electrical response of PPy nanotubes upon periodic exposure to NH_3 vapor of 20 ppm. As PPy nanotubes were exposed to NH_3 vapor, the rapid increment in resistance (positive normal resistance changes) was observed. After the NH_3 flow was replaced by compressed air flow, the conductivity of PPy nanotubes was observed to slowly recover due to the desorption of NH_3 molecules from the nanotubes. The cyclic tests presented similar responses more than five times. These facts suggest that PPy nanotubes can be reversibly used in detecting NH_3 vapor. Provided residual NH_3 molecules were trapped in PPy nanotubes, irreversible responses could be observed. However, the nanometer-sized wall (approximately 20−50 nm thickness) of PPy nanotubes allows the fast diffusion of NH_3 molecules in and out of the polymer. Figure 3b illustrates the response of PPy nanotubes upon sequential exposures to NH_3 vapors of three different concentrations (20, 50, and 100 ppm). The PPy nanotube sensors showed reversible and reproducible responses for each vapor concentration, and their responses were more pronounced with increasing vapor concentration. These facts suggest that PPy nanotubes can be effectively utilized in detecting NH_3 vapor of various concentrations. Figure 3c plots the sensitivity change of PPy nanotubes as a function of NH_3 vapor concentration. PPy nanotubes showed much larger sensitivity (>10-fold) than their bulky PPy counterpart. It can be explained that the nanostructured PPy provides a high surface-to-volume ratio. At low concentrations (<10 ppm), the PPy nanotube sensors showed nonlinear behavior in sensitivity change, because the normalized resistance change should be zero at 0 ppm. On the other hand, linear behavior could be observed over a wide concentration range of 10−100 ppm. Linear regression fits to the data-point range

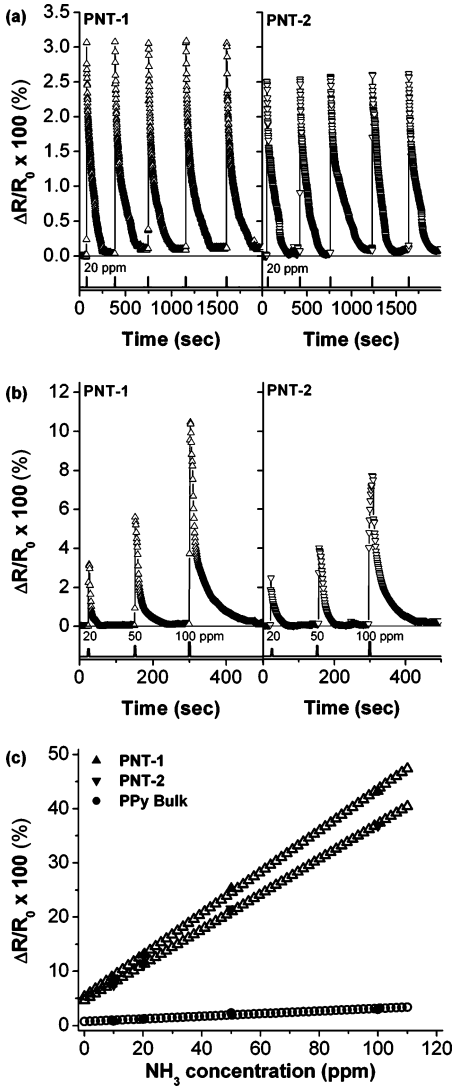

Figure 3. (a) Responses of PPy nanotubes upon periodic exposure to NH_3 vapor of 20 ppm. (b) Responses of PPy nanotubes upon sequential exposure to NH_3 vapor of 20, 50, and 100 ppm. (c) Sensitivity changes of PPy nanotubes as a function of NH_3 vapor concentration.

yielded the following equations (calibration curves) for two different PPy nanotubes:

$$\text{PNT-1} \qquad y\,(\%) = 0.382x\,(\text{ppm}) + 5.356 \qquad (2)$$

$$\text{PNT-2} \qquad y\,(\%) = 0.325x\,(\text{ppm}) + 4.659 \qquad (3)$$

The sensitivity of PNT-1 was always better than that of PNT-2 upon exposure to NH_3 vapors of various concentrations. The smaller dimensions of PNT-1 provide a higher surface area as well as faster analyte diffusion. The Raman (Figure 2) spectra also revealed that PNT-1 has a higher oxidation level and a longer conjugation length than PNT-2. These facts gave rise to more sensitive responses in PNT-1 than in PNT-2.

In general, the change in resistance under UV illumination can be related to photoconductivity, i.e., an electrical phenomenon in which a material becomes more conductive when subjected to electromagnetic radiation. For one carrier, photoconductivity (σ_p) is given by the expression

$$\sigma_p = \sigma_i - \sigma_d = e\mu\Delta n + en\Delta\mu \qquad (4)$$

where e is the unit charge, n is the density of free charge carriers, and μ is their mobility. σ_i and σ_d are the electrical conductivity

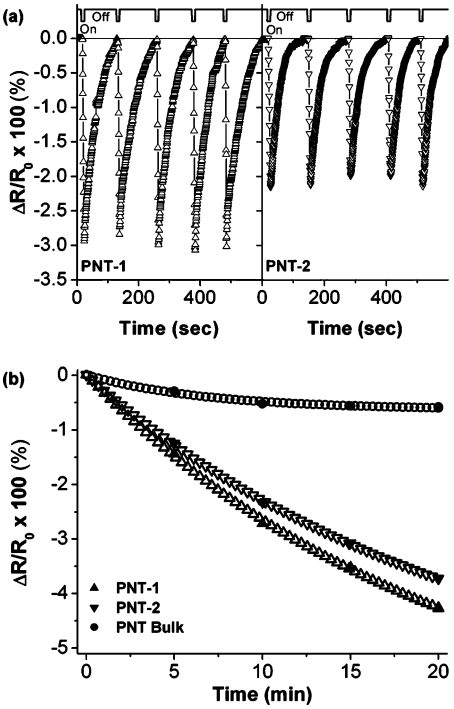

Figure 4. (a) Responses of PPy nanotubes upon periodic UV illumination (10 s duration). (b) Photosensitivity changes of PPy nanotubes as a function of UV illumination time.

under illumination and in the dark, respectively. In other words, photoconductivity is dependent on the change of free charge carriers in density and mobility.

To investigate the response of PPy nanotubes under UV illumination, PPy nanotubes were repeatedly exposed to UV light and the resistance changes were monitored in real time (Figure 4a). When the PPy nanotubes were illuminated with UV light, the resistance kept dropping (negative normalized resistance change). After the light was off, the resistance slowly recovered to the original level. The drop in resistance (namely, the rise in conductivity) of PPy nanotubes under UV illumination can be understood in terms of the following two respects: (i) the photogeneration of free charge carriers in the nanotubes via processes such as dissociation of excitons at PPy/electrode interface, autoionization of excitons, and direct band-to-band transition; (ii) the mobility variation of charge carriers from heating the nanotubes with photon adsorption. On the basis of these mechanisms, the conductivity of PPy nanotubes grew with the UV light exposure and decayed slowly when the light was off. The PPy nanotubes underwent five on−off cycles and gave similar responses in each cycle, indicating that the reversibility and reproducibility of the nanotube sensors were excellent.

In Figure 4a, PNT-1 responded with a larger intensity than PNT-2 in decreasing resistance. To further elucidate the influence of the nanotube diameter on the sensitivity of PPy nanotubes, the photosensitivity change of PPy nanotubes was plotted against illumination time in Figure 4b. Both PPy nanotubes revealed more improved responses when irradiated with UV light for a longer time. During the illumination regime, nonlinear behaviors were observed in the response of PPy nanotubes, and the sensitivity of PPy nanotubes followed an exponential relationship in the illumination time range of 5−20 s:

$$\text{PNT-1} \qquad y\,(\%) = 6.755\,\exp[-0.050x\,(\text{s})] - 6.755 \qquad (5)$$

$$\text{PNT-2} \qquad y\,(\%) = 6.128\,\exp[-0.047x\,(\text{s})] - 6.128 \qquad (6)$$

PPy nanotubes showed larger responses (>10-fold) compared with PPy bulk. Moreover, PNT-1 showed a more pronounced response than PNT-2. Therefore, it is clear that the photosensitive response of PPy nanotubes under UV illumination is fairly dependent on their dimensions. The result is in accord with the response of PPy nanotubes upon exposure to NH_3 vapors. Under our experimental conditions, it was evident that PNT-1 with a smaller diameter was more sensitive than PNT-2 due to its longer conjugation length and larger surface area.

Conclusions

For both NH_3 vapor and UV light, the electrical response of PPy nanotubes was strongly dependent on their diameters. In addition, the nanotube sensors showed improved performance compared with their bulky counterpart. The ability to perceive chemical vapor and electromagnetic radiation may provide the feasibility for multifunctional sensors,[29−35] and could be expanded to potential applications in the fields of actuators, transistors, switches, resistors, and memory cells.[36]

Acknowledgment. This work was financially supported by the Brain Korea 21 program of the Korean Ministry of Education, and the Hyperstructured Organic Materials Research Center is supported by the Korea Science and Engineering Foundation.

References and Notes

(1) Janata, J.; Josowicz, M. *Nat. Mater.* **2003**, *2*, 19.
(2) McQuade, D. T.; Pullen, A. E.; Swager, T. M. *Chem. Rev.* **2000**, *100*, 2537.
(3) Albert, K. J.; Lewis, N. S.; Schauer, C. L.; Sotzing, G. A.; Stitzel, S. E.; Vaid, T. P.; Walt, D. R. *Chem. Rev.* **2000**, *100*, 2595.
(4) Ameer, Q.; Adeloju, S. B. *Sens. Actuators, B* **2005**, *106*, 541.
(5) Wang, Y.; Sotzing, G. A.; Weiss, R. A. *Chem. Mater.* **2003**, *15*, 375.
(6) Li, G.; Martinez, C.; Semancik, S. *J. Am. Chem. Soc.* **2005**, *127*, 4903.
(7) Wang, J.; Chan, S.; Carlson, R. R.; Luo, Y.; Ge, G.; Ries, R. S.; Heath, J. R.; Tseng, H.-R. *Nano Lett.* **2004**, *4*, 1693.
(8) Forzani, E. S.; Zhang, H.; Nagahara, L. A.; Amlani, I.; Tsui, R.; Tao, N. *Nano Lett.* **2004**, *4*, 1785.
(9) Jang, J.; Chang, M.; Yoon, H. *Adv. Mater.* **2005**, *17*, 1616−1620.
(10) Virji, S.; Fowler, J. D.; Baker, C. O.; Huang, J.; Kaner, R. B.; Weiller, B. H. *Small* **2005**, *1*, 624.
(11) Huang, J.; Virji, S.; Weiller, B. H.; Kaner, R. B. *J. Am. Chem. Soc.* **2003**, *125*, 314.
(12) Liu, J.; Lin, Y.; Liang, L.; Voigt, J. A.; Huber, D. L.; Tian, Z. R.; Coker, E.; Mckenzie, B.; Mcdermott, M. J. *Chem.—Eur. J.* **2003**, *9*, 604.
(13) Liu, H.; Kameoka, J.; Czaplewski, D. A.; Craighead, H. G. *Nano Lett.* **2004**, *4*, 671.
(14) Dong, B.; Zhong, D.; Chi, L.; Fuchs, H. *Adv. Mater.* **2005**, *17*, 2736.
(15) Martin, C. R. *Acc. Chem. Res.* **1995**, *28*, 61.
(16) Hermsdorf, N.; Stamm, M.; Förster, S.; Cunis, S.; Funari, S. S.; Gehrke, R.; Müller-Buschbaum, P. *Langmuir* **2005**, *21*, 11987.
(17) Jang, J.; Ko, S.; Kim, Y. *Adv. Funct. Mater.* **2006**, *16*, 754.
(18) Jang, J.; Bae, J. *Adv. Funct. Mater.* **2005**, *15*, 1877.
(19) Han, M. G.; Foulger, S. H. *Chem. Commun.* **2005**, 3092.
(20) Jang, J.; Bae, J. *Angew. Chem., Int. Ed.* **2004**, *43*, 3803.
(21) Jang, J.; Yoon, H. *Adv. Mater.* **2004**, *16*, 799.
(22) Jang, J.; Yoon, H. *Adv. Mater.* **2003**, *15*, 2088.
(23) Yang, X.; Zhu, Z.; Dai, T.; Lu, Y. *Macromol. Rapid Commun.* **2005**, *26*, 1736.
(24) Jang, J.; Yoon, H. *Chem. Commun.* **2003**, 720.
(25) Hulvat, J. F.; Stupp, S. I. *Angew. Chem., Int. Ed.* **2003**, *42*, 778.
(26) Carswell, A. D. W.; O'Rear, E. A.; Grady, B. P. *J. Am. Chem. Soc.* **2003**, *125*, 14793.
(27) Jang, J.; Yoon, H. *Langmuir* **2005**, *21*, 11484.
(28) Dauginet-De Pra, L.; Demoustier-Champagne, S. *Polymer* **2005**, *46*, 1583.
(29) Wei, C.; Dai, L.; Roy, A.; Tolle, T. B. *J. Am. Chem. Soc.* **2006**, *128*, 1412.
(30) Liu, Z.; Searson, P. C. *J. Phys. Chem. B* **2006**, *110*, 4318.
(31) Shi, L.; Yu, C.; Zhou, J. *J. Phys. Chem. B* **2005**, *109*, 22102.
(32) Cho, J.-H.; Yu, J.-B.; Kim, J.-S.; Sohn, S.-O.; Lee, D.-D.; Huh, J.-S. *Sens. Actuators, B* **2005**, *108*, 389.
(33) Grancharov, S. G.; Zeng, H.; Sun, S.; Wang, S. X.; O'Brien, S.; Murray, C. B.; Kirtley, J. R.; Held, G. A. *J. Phys. Chem. B* **2005**, *109*, 13030.
(34) Gao, L.; Fang, Y.; Wen, X.; Li, Y.; Hu, D. *J. Phys. Chem. B* **2004**, *108*, 1207.
(35) Bekyarova, E.; Davis, M.; Burch, T.; Itkis, M. E.; Zhao, B.; Sunshine, S.; Haddon, R. C. *J. Phys. Chem. B* **2004**, *108*, 19717.
(36) Jang, J. *Adv. Polym. Sci.* **2006**, *199*, 189.